

## COLLAPSE CAPACITY ASSESSMENT OF REGULAR TALL BUILDINGS UNDER PULSE LIKE NEAR FIELD GROUND MOTIONS

Ali SAFFAR

Graduate student, Civil Engineering Department, Sharif University of Technology-International Campus,  
Kish Island, Iran  
saffar@kish.sharif.edu

Fayaz R. ROFOOEI

Professor, Civil Engineering Department, Sharif University of Technology, Tehran, Iran  
rofooei@sharif.edu

**Keywords:** Collapse Capacity, Tall Buildings, Pulse-Like Ground Motions, Forward Directivity,

### ABSTRACT

Structural response to near fault ground motions has received significant attention in recent years. Such ground motions are different from ordinary ones and are characterized by a large, long period, velocity pulse caused by the forward directivity. These velocity pulses could potentially impose severe demands on structures and increase their risk of seismic collapse. The situation could even be worse for tall buildings with fundamental periods close to the period of the velocity pulses, and requires special consideration in design process. Besides, Prediction of seismic-induced collapse potential of structures has been among the main concerns in Performance Based Earthquake Engineering (PBEE). The results could be used as an important measure in designing new structures, or evaluating the seismic performance of existing ones. Not surprisingly, much effort has been made in accurate prediction of collapse capacity of structures due to its importance in estimation of the human and monetary losses during and after an earthquake episode. Collapse assessment of structure under near fault directivity excitation shows a higher value than expected by the code which is 1% in 50 years but in the case of the farfield suites the results are almost consistent with the design collapse level defined by the code.

### INTRODUCTION

In this paper the collapse capacity of regular tall buildings under near-field ground motions with directivity effect will be investigated. A number of building models with different number of stories is considered. Using a sufficient number of near field ground motions suggested by Baker (2007), from PEER NGA database, the effect of near fault ground motion on the models is evaluated. In order to recognize the strong pulse in velocity time history, all the pulse like ground motion in database have been rotated to the fault normal direction. Seismic collapse risk of each archetype building is evaluated using incremental dynamic analysis (IDA) Vamvatsikos D, Cornell C. Allin (2002). Also, the procedure is repeated for the far field earthquake excitation to compare the effect of near field and far field earthquake excitation on collapse capacity of tall buildings. The far-field database is based on the FEMA P695 ground motion set. This work is a part of a comprehensive research on collapse capacity of irregular tall buildings subjected to near-field ground motions. The hypothetical site of the buildings is located in downtown Los Angeles, California, USA with the longitude = -118.25 and latitude = 34.05 that is near to several known faults.

In order to evaluate the collapse risk of the structures, this study utilizes the  $c$  which is then used to calculate the probability of collapse of the buildings in 50 years. It then will be possible to estimate the collapse potential of buildings that fulfill the ASCE7-10 target design collapse level which is 1% in the 50 years. Seismic hazard curves and collapse fragility curves of buildings are two main components to compute the  $c$ .

## GROUND MOTION DATABASES

Two suits of earthquake records are used in this study in order to evaluate the seismic collapse risk of buildings. The first include 14 pulse like strong ground motions listed by Baker (Baker 2007). Baker used wavelet analysis to quantitatively identify the presence of the directivity pulses in those records. Wavelet analysis decomposes a complex signal, such as ground motion record, into a summation of basis functions referred to as wavelets. Once a pulse is identified, it can be extracted from the original record by means of wavelet decomposition, thus leaving the residual ground motion. The size of the extracted pulse relative to the residual ground motion indicates the significance of the pulse and can be used to classify the suite of near-fault records. By examining the dominant frequency of the wavelet form, the period of the detected velocity pulses can be evaluated. A complete list of near-fault ground motions used in this study is presented in the Table. The records include a range of pulse period,  $T_p$ , varying from 0.4 to 5.7s. These ground motions were recorded from earthquake events with moment magnitudes ( $M_w$ ) ranging from 5.2 to 7.6, with an average magnitude of 6.4. The peak ground velocity (PGV) is listed for each record with values ranging from 30.4 cm/sec to 169.9 cm/sec. The site-to-source distances are also included in Table 5.1 with epicentral distances ranging approximately from 2.5 km to 38.6 km and an average value of 17.3 km. All of the records in the data base have been rotated to fault normal direction.

The second data set which contains the far field, non-pulse like ground motions is selected based on FEMA p695 (FEMA 2009). All these ground motions are consistent with soil type D.

Table 1: Near-field ground motion records database

#	Earthquake			Recorded Motion			Distance	
	Event	Station	Year	$M_w$	$T_p$ Wavelet	PGV	Closest D.	Epi. D.
1	Imperial Valley-06	Aeropuerto Mexicali	1979	6.5	2.4	44.3	0.3	2.5
2	Imperial Valley-06	El Centro Array #6	1979	6.5	3.8	111.9	1.4	27.5
3	Imperial Valley-06	El Centro Array #7	1979	6.5	4.2	108.8	0.6	27.6
4	Mammoth Lakes-06	Long Valley Dam (Upr L Abut)	1980	5.9	1.1	33.1	16	14
5	Westmorland	Parachute Test Site	1981	5.9	3.6	35.8	16.7	20.5
6	Coalinga-07	Coalinga-14th & Elm (Old CHP)	1983	5.2	0.4	36.1	10.9	9.6
7	N. Palm Springs	North Palm Springs	1986	6.1	1.4	73.6	4	10.6
8	Whittier Narrows-01	Downey - Co Maint Bldg	1987	6	0.8	30.4	20.8	16
9	Superstition Hills-02	Parachute Test Site	1987	6.5	2.3	106.8	1	16
10	Erzican, Turkey	Erzincan	1992	6.7	2.7	95.4	4.4	9
11	Northridge-01	Rinaldi Receiving Sta	1994	6.7	1.2	167.2	6.5	10.9
12	Kobe, Japan	Takarazuka	1995	6.9	1.4	72.6	0.3	38.6
13	Kobe, Japan	Takatori	1995	6.9	1.6	169.6	1.5	13.1
14	Chi-Chi, Taiwan	TCU065	1999	7.6	5.7	127.7	0.6	26.7

## BUILDING DESIGN AND SIMULATION MODEL

The framing systems used for the structural models in this study are space and perimeter frames. The steel structures considered in this study are idealized using two dimensional, five bay frames with variable heights ranging from 60 to 100 meters. Structural models are designed for vertical and lateral loads in accordance with LRFD specifications, SEI/ASCE-07-10 (Engineers 2010) and ANSI/AISC 360-10 (AISC 2010) design provisions. The buildings are assumed to be located in downtown Los Angeles, CA, USA and are office building with movable partitions. The hinges for the beam and columns was defined using the ASCE 41-06 guidelines (ASCE 2007).

The plan view of the models is shown in Figure 1. The structural system is a special moment resisting frame (SMRF) because this lateral-load resisting system is typical in seismic-prone areas. Columns are fixed at the base level. The buildings stories are 4 meters high with a bay equal to 6 meters. A992 Grade 50 steel is specified for the beams while A500 Grade B46 steel was considered for the columns. For the space and perimeter frames the A992 Grade 50 steel were used. The assumed dead loads of the buildings is 6.5 kN/m<sup>2</sup> and the live load for the office building considered as 2.5 kN/m<sup>2</sup> according to SEI/ASCE-07-10 (ASCE 2010). The focus is on the east west (EW) loading direction. As it was mentioned before, the structural models used in this study were designed for a hypothetical site in downtown Los Angeles, Ca, USA (longitude=-118.25 and latitude=34.05). The soil conditions are consistent with those of site class D. The



site is close to several Known Faults, Including the Puente Hills and San Andreas faults, respectively at close distances of 1.5 and 56 km from the building site (Yang, Moehle et al. 2012). The maximum considered earthquake (MCE) spectral response acceleration at short periods  $S_s$  and at 1 second period ( $S_1$ ) is assumed to be 2.402g and 0.843g, respectively. They were specified using the zonation maps provided by ASCE/SEI 7-10 (Engineers 2010) and confirmed using the United States Geological Survey (USGS) website (USGS 2014 [Online]) for the assumed location. The design spectral response acceleration parameters  $S_{DS}$  and  $S_{D1}$  are 1.601 and 0.843 respectively.

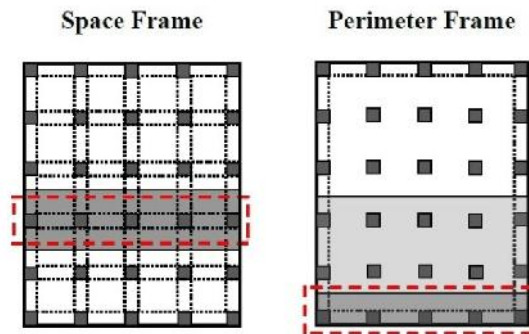


Figure 1 The tributary areas for lateral and gravity loads for the space and perimeter frame systems.

## COLLAPSE CAPACITY ASSESSMENT PROCEDURE

Generally collapse potential of structure is related to the structural response parameter (i.e. story drift ratio or roof drift ratio). The element type utilized in modeling the building structures, the computer program used to analysis, and modeling assumption are parameters which effect the structural response (Ibarra and Krawinkler 2005). Therefore, the buildings collapse capacity is straightly determined based on ground motion intensity which leads to dynamic instability of the structural model (Zareian and Krawinkler 2006, Zareian and Krawinkler 2007). In order to obtain the collapse capacity for each ground motion, incremental dynamic analysis (IDA) (Vamvatsikos and Cornell 2002) is employed. Performing the nonlinear time history analysis and increasing the  $S_a(T_1, 5\%)$  of the ground motion would eventually lead to the intensity level at which the structure become dynamically instable. This process is shown in the Figure 2 for 15 story building moment resisting frame subjected to near fault ground motion data set. The colored circle at the end of each IDA curve which is projected on the vertical axis, shows the last point at which the solution converged.

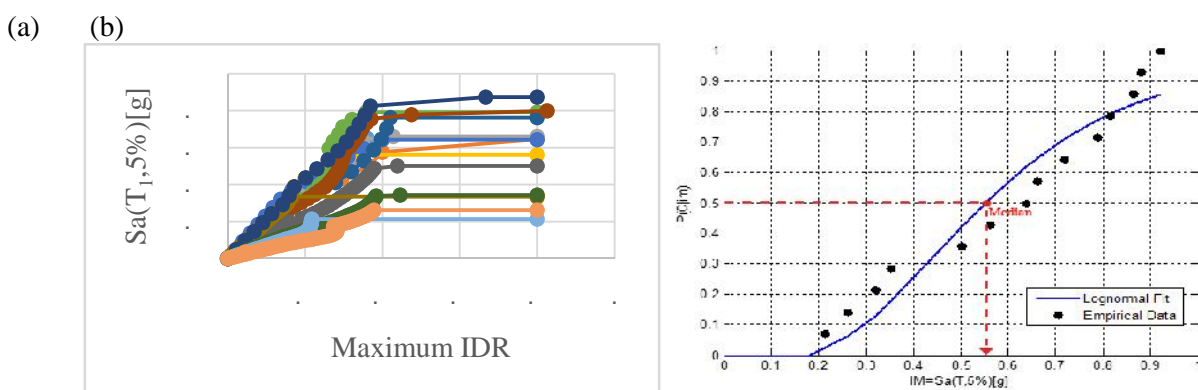


Figure 2 Obtaining the collapse fragility curve with Incremental Dynamic Analysis:  
a) obtaining data point, b) collapse fragility curve

The uncertainty exists in calculations of structural behavior and seismic risk may be categorized into one of two conceptual types: aleatory or epistemic. Aleatory uncertainty refers to some phenomenon that is inherently random and cannot be reduced. Epistemic uncertainty, alternatively, refers to the uncertainty resulting from lack of knowledge or erroneous modeling techniques. In contrast to aleatory uncertainty,

epistemic uncertainty can be reduced with additional research and a better understanding of the event being modeled (Mavroeidis, Dong et al. 2004).

The uncertainty considered in this study accounts for record-to-record variability and structural modeling uncertainties. Record-to-record variability is recognized to variations in the ground motion characteristics and is considered aleatory. While naturally random, this type of uncertainty can be precisely quantified by computing the scattering of the results from incremental dynamic analysis. Modeling uncertainty relates to the variation in the actual physical properties and seismic response of a structure. This source of uncertainty stems from the definition of the structural model parameters, such as strength, stiffness and deformation capacity, and is especially important for predicting structural collapse (Liel, Haselton et al. 2009). The mean estimate procedure combines the relative contributions of record-to-record (RTR) variability and modeling uncertainties to compute the total variance of the structural response fragility. The total variance is taken as the square root of the sum of the squares of the discrete uncertainties, as seen in Eq. (1). This approach assumes that both sources of uncertainty can be designated using a lognormal distribution and that they are independent of one another. When the mean estimate approach utilized the median remains unchanged but the variance of the collapse fragility increases. A standard deviation of 0.25 for uncertainty in analytical computation of global collapse was used for the dashed curve in accordance to FEMA-351 (Committee, California et al. 2000) for steel high rise structures.

$$(\tau_{LN}) = \sqrt{(\tau_{LN})_{RTR}^2 + (\tau_{LN})_{Model}^2} \quad (1)$$

In order to evaluate the collapse risk of structures this study uses  $\lambda_c$ . Calculation of  $\lambda_c$  need two elements: the seismic hazard curve, which gives the mean annual frequency of exceeding ground motion intensity at the site, and the collapse fragility curves of the structures, which represent the collapse probability of structure's due to the intensity of the ground motion. As mentioned before, the intensity of ground motion is quantified by an IM such as  $Sa(T1,5\%)$ , 5% damped spectral acceleration at the first mode period of structure.

Utilizing the following equation, the mean annual frequency of collapse is estimated through the convolution of structure collapse fragility curve from incremental dynamic analysis over the site-specific ground motion hazard curve (Deierlein 2004, Ibarra and Krawinkler 2005, Zareian and Krawinkler 2006), as shown below;

$$\lambda_c = \int_0^{\infty} P(C|im) \cdot d\lambda_{IM}(im) \quad (2)$$

Where  $P(C|im)$  represents the probability at which the structure will collapse due to an earthquake with the intensity level IM. The cumulative distribution function, CDF, which corresponds to fragility curve, is either derived to account for only aleatory uncertainty or aleatory and epistemic uncertainty. The parameter  $\lambda_{IM}$  is defined as the mean annual frequency of exceedance of the ground motion intensity, IM. Equation 2 can be rewritten when multiplying and dividing the right hand side of the equation by  $d(im)$ . The re-written equation is represented below,

$$\lambda_c = \int_0^{\infty} P(C|im) \cdot \left| \frac{d\lambda_{IM}(im)}{d(im)} \right| \cdot d(im) \quad (3)$$

Where  $d\lambda_{IM}(im)/d(im)$  is the slope of the seismic hazard curve at the site. Generally, this integral can be solved using numerical integration because there is no closed form solution to solve it. Although, Jalayer and Cornell (Cornell, Jalayer et al. 2002, Jalayer 2003) suggested a closed form solution to approximate the probabilistic collapse assessment. Regarding to Eads et al. (Eads, Miranda et al. 2013), the integral can be solved numerically by computing the product of the collapse probability conditioned on IM, i.e.,  $Sa(T1,5\%)$ , and the seismic hazard curve slope at discrete IMs, multiplying by the increment in IM ( $\Delta im$ ) and summing the result from all IMs. Equation 4 representing the process discussed above.

$$\lambda_c = \sum_0^{\infty} P(C|im) \cdot \left| \frac{d\lambda_{IM}(im)}{d(im)} \right| \cdot \Delta(im) \quad (4)$$



## PROBABILITY OF COLLAPSE AND $\alpha_c$ CONNECTION

The mean rate of collapse of the building in a year computed by  $\alpha_c$ . The probability of collapse of a structure through  $n$  years can be evaluated by the following equation if the earthquake occurrence is assumed to follow a Poisson distribution,

$$P_c(\text{in } n \text{ years}) = 1 - \exp(-\alpha_c n) \quad (5)$$

Collapse annual probability can be roughly considered identical to  $\alpha_c$  by virtue of the value of  $\alpha_c$  is small for common structures. Collapse probability for both the near-fault (N-F) and far-field (F-F) are presented in

$$P_c(\text{in 1 year}) \cong \alpha_c \quad (6)$$

Table 2: Collapse prediction for models

ID	T(s)	$\mu$	RTR		RTR + Model		$\alpha^*$
			P[C] F-F	P[C] N-F	P[C] F-F	P[C] N-F	
15 Space	2.49	0.55	0.0088	0.0172	0.009	0.0197	0.323
15 Perimeter	2.52	0.61	0.009	0.0191	0.0094	0.0226	0.35
20 Space	3.14	0.354	0.008	0.0299	0.0081	0.0338	0.176
20 Perimeter	3.2	0.4	0.0083	0.0406	0.0089	0.0441	0.21
25 Space	3.8	0.329	0.009	0.0182	0.0092	0.0207	0.165
25 Perimeter	3.85	0.35	0.0093	0.0304	0.0095	0.0367	0.19
Average		0.432	0.0087333	0.0259	0.00902	0.036033	0.236

$\alpha^*$  = The maximum value in the  $\alpha_c$  deaggregation

## $\alpha_c$ DEAGGREGATION

$\alpha_c$  computed by Eq. 4 aggregate the result of multiplication of the fragility curve by the slope of hazard curve at all the intensities. So, it might come to mind “which intensity has the most contribution in collapse of the characteristic building?!”. The answer to this question can be evaluated through the deaggregation of  $\alpha_c$  which is less than the median shown in Figure 4 for the near fault data base.

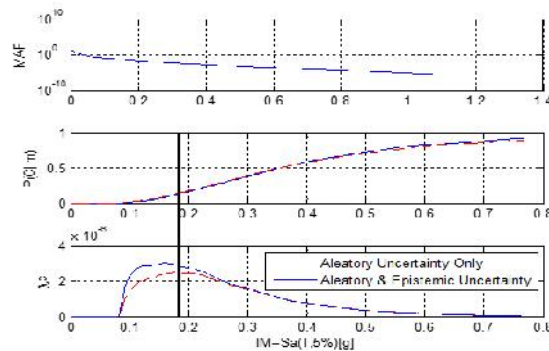


Figure 3 illustrated the result of  $\alpha_c$  deaggregation for the 20 moment resisting frame models for both the record to record variability (aleatory uncertainty) and record to record and model variability (aleatory and epistemic uncertainty) for the near-fault database. This procedure is similar to the probabilistic seismic hazard analysis deaggregation which defined by Bazzurro and Cornell (Bazzurro and Cornell 1999). Regarding the  $\alpha_c$  deaggregation, the maximum value in which is less than the median shown in Figure 4 for the near fault data base.



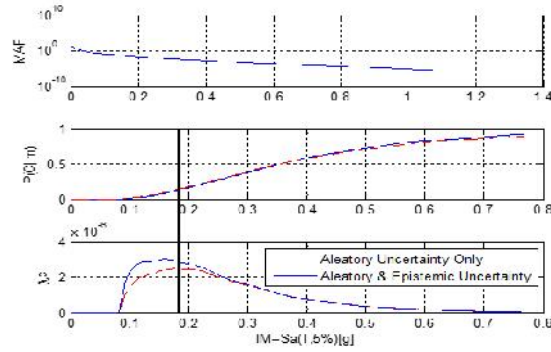


Figure 3 which corresponds to the highest collapse risk contribution happens when  $Sa(T1=3.14,5\%)$  equals 0.1765 for aleatory uncertainty (illustrated by vertical line in which is less than the median shown in Figure 4 for the near fault data base).

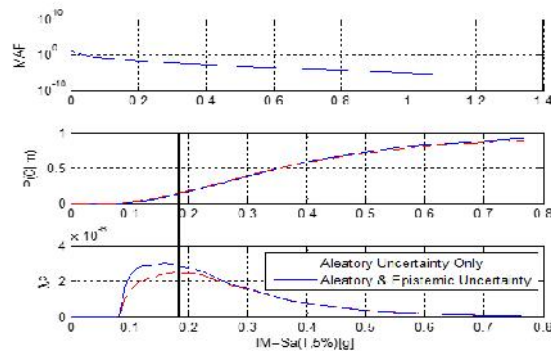


Figure 3) which is related to the collapse probability of approximately 11%. As expected, the building collapse risk dominated by the intensities corresponding to the lower half of collapse fragility curve which is less than the median shown in Figure 4 for the near fault data base.

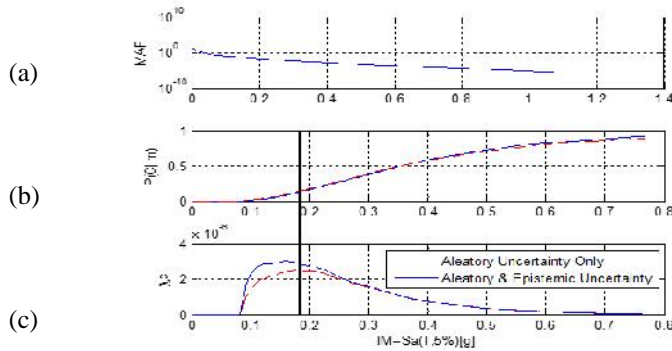


Figure 3:20 Space collapse risk assessment: (a) slope of seismic hazard curve, (b) collapse fragility curves, and (c)  $\lambda$  deaggregation curves.

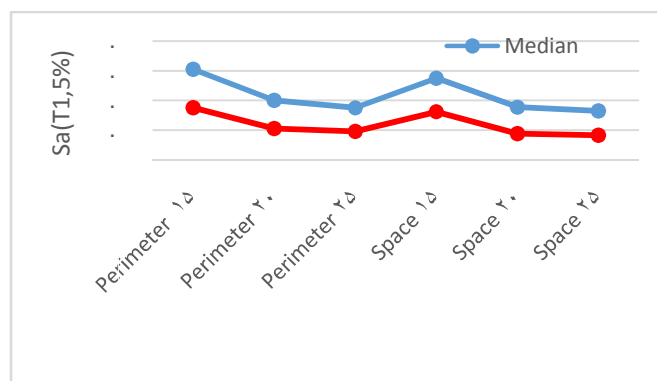


Figure 4: Deaggregation and median of collapse comparison for the near-field ground motion data base

## CONCLUSIONS

In this study the effect of the near-field ground motions on the seismic collapse capacity of the structures are examined. The results presented in the followings are based on the limitation of the study and the assumption used. It is clear that due to the random nature of the earthquake ground motions and assumption used in the design of the structures, the result might be varying if any of the assumptions are changed.

A group of 6 Steel moment frame used in this study with 15,20 and 25 stories ranging from 60 to 100 meters height representing the high rise steel moment resisting frames. The structures are designed for the hypothetical site in the Los Angeles, CA. The site is selected to be near to several known fault in the California in order to better illustrate the performance evaluation of the structures designed for the near field regions based on the most US seismic provisions. The special steel moment resisting frame, SMRF, used as the lateral load resisting elements of all of the studied buildings.

A probabilistic seismic collapse assessment is performed that is computed by means of the mean annual frequency of collapse, which is then utilized to evaluate the building collapse probability in 50 years. In order to evaluate the mean annual frequency of collapse, the slope of the seismic hazard curve for the hypothetical site combined by the collapse probability of the building conditioned on intensity measure along with the increment of the IM, and the summation of the outcomes of all the IMs. Epistemic and aleatory types of uncertainty have been considered in this study. A suite of the 14 pulse like ground motions that are consistent with soil type D are selected for this study.

Regarding to deaggregation results it can be concluded that intensities corresponding to the lower half of collapse fragility curve commonly dominate the collapse risk. So, it might be better to put emphasis on the lower half of collapse fragility curve, especially on those intensities determined from the deaggregation of  $\rho_c$  that have large contribution to the collapse capacity, instead of considering the median collapse intensity.

Based on the observation made in this study it can be concluded that a detailed collapse risk assessment in the near-fault site is vital to develop and improve the seismic hazard maps and the structural design criteria. Current seismic provision utilizes the MCER in order to compute the base shear for design of the building. Before the 2010 edition of ASCE7 and the 2012 edition of the IBC the MCE was considered as ground motion intensity which has 2% probability of collapse in 50 years. But the updated version of ASCE 7 and IBC, suggest new risk-target design maps, that represent the new quantity, MCER, a uniform target probability. In order to define the MCER a uniform collapse probability approximately 1% in 50 years is considered for the region throughout the US. Notwithstanding the change to new risk-targeted procedure, the seismic hazard maps that shows the risk of collapse in the near-fault site do not clearly reflected in the new seismic hazard maps. Based on the limited result of this study it can be seen that the collapse risk of the structures designed based on the most current US seismic provisions in the near-fault site do not fulfill the target design collapse risk level which is 1% in the 50 years. The effects of forward directivity may leads to an increase in the collapse risk of the structures.

## REFERENCES

AISC (2010) Specification for Structural Steel Buildings, ANSI/AISC 360-10; American Institute of Steel Construction Chicago, IL, USA

ASCE (2007) Seismic Rehabilitation of Existing Buildings, American Society of Civil Engineers

ASCE (2010) Minimum Design Loads for Buildings and Other Structures: Second Printing, American Society of Civil Engineers

Baker JW (2007) Quantitative classification of near-fault ground motions using wavelet analysis. Bulletin of the Seismological Society of America 97(5): 1486-1501

Bazzurro P and Cornell CA (1999) Disaggregation of seismic hazard. Bulletin of the Seismological Society of America 89(2): 501-520

Committee SJVGD et al. (2000) Recommended seismic evaluation and upgrade criteria for existing welded steel moment-frame buildings, Fema



- Cornell CA et al. (2002) Probabilistic basis for 2000 SAC federal emergency management agency steel moment frame guidelines. *Journal of Structural Engineering* 128(4): 526-533
- Deierlein G (2004) Overview of a comprehensive framework for earthquake performance assessment. Performance-Based Seismic Design Concepts and Implementation, Proceedings of an International Workshop
- Eads L et al. (2013) An efficient method for estimating the collapse risk of structures in seismic regions. *Earthquake Engineering & Structural Dynamics* 42(1): 25-41
- Engineers ASC (2010) Minimum Design Loads for Buildings and Other Structures: Second Printing, American Society of Civil Engineers.
- FEMA (2009) Quantification of Building Seismic Performance Factors, FEMA P695, Washington, DC.
- Ibarra LF and Krawinkler H (2005) Global collapse of frame structures under seismic excitations, Pacific Earthquake Engineering Research Center.
- Jalayer F (2003) Direct probabilistic seismic analysis: implementing non-linear dynamic assessments, Stanford University
- Liel AB et al. (2009). Incorporating modeling uncertainties in the assessment of seismic collapse risk of buildings. *Structural Safety* 31(2): 197-211
- Mavroeidis G et al. (2004) Near-fault ground motions, and the response of elastic and inelastic single-degree-of-freedom (SDOF) systems. *Earthquake Engineering & Structural Dynamics* 33(9): 1023-1049
- USGS (2014[Online]) U.S. Geological Survey Earthquake Hazard Program Available: <http://earthquake.usgs.gov/hazards>
- Vamvatsikos D and Cornell CA (2002) Incremental dynamic analysis. *Earthquake Engineering & Structural Dynamics* 31(3): 491-514
- Yang T et al. (2012) Performance assessment of tall concrete core-wall building designed using two alternative approaches. *Earthquake Engineering & Structural Dynamics* 41(11): 1515-1531
- Zareian F and Krawinkler H (2006) Simplified Performance-Based Earthquake Engineering, Stanford University
- Zareian F and Krawinkler H (2007) Assessment of probability of collapse and design for collapse safety. *Earthquake Engineering & Structural Dynamics* 36(13): 1901-1914

